

Effects of head model inaccuracies on regional scalp and skull conductivity estimation using real EIT measurements

M. Fernández-Corazza^{1,2,3}, S. Turovets^{4,5}, P. Govyadinov⁶, C.H. Muravchik^{1,7} and D. Tucker^{4,5}

¹ LEICI - Instituto de Electrónica, Control y Procesamiento de Señales, Facultad de Ingeniería, UNLP, Buenos Aires, Argentina.

² Consejo Nacional de Investigaciones Científicas y Técnicas (CONICET), Argentina

³ Departamento de Ciencias Básicas, Facultad de Ingeniería, UNLP, Buenos Aires, Argentina.

⁴ NeuroInformatics Center, University of Oregon, Eugene, OR, USA

⁵ Electrical Geodesics Inc. (EGI), Eugene, OR, USA.

⁶ Electrical and Computer Engineering, University of Huston, TX, USA

⁷ Comisión de Investigaciones Científicas de la Provincia de Buenos Aires (CICpBA), Buenos Aires, Argentina.

Abstract— Parametric or bounded Electrical Impedance Tomography (bEIT) is a combination of EIT with structural magnetic resonance (MR) for the parametric estimation of the electrical conductivity of the main tissues of the head. The better conductivity values improve accuracy of realistic electrical head models used in source localization in electroencephalography (EEG), or in the emerging transcranial electrical stimulation (tDCS) therapies. Based on real bEIT measurements on two healthy adults, and using 62 current injection pairs of a high dense 128 sensor array, we compare the estimations of the scalp and skull conductivities within three different electrode models: pointwise, volumetric, and the Complete Electrode Model (CEM). We also analyze the influence of the skull holes and the cerebrospinal fluid (CSF). The scalp (skull) conductivity for these two subjects were estimated to be ~ 0.4 and ~ 0.3 S/m (~ 0.0045 and ~ 0.005 S/m). The results were similar for all three electrode models ($< 8\%$), but volumetric and CEM models resulted in a better fitting to real data. A model of nested and closed surfaces (no skull holes) resulted in a significant overestimation ($\sim 23\%$) of the skull conductivity. Moreover, neglecting the CSF resulted in an extra 28% overestimation of the skull conductivity.

Keywords— bounded electrical impedance tomography, electrode modelling, complete electrode model, parametric estimation, skull conductivity.

I. INTRODUCTION

In Electrical Impedance Tomography (EIT), an electric current is applied on the boundary of a conductive object and the resulting potentials are measured by a sensor array on the object's surface. These measurements can be used to estimate the electrical conductivity distribution in the interior of the object. The clinical applications of EIT are numerous, from lung perfusion monitoring to breast cancer detection [1]. EIT is considered to have a

great potential in medical diagnostics as it is a portable, low-cost and non-invasive technique [1]. When applied to the human head, it can be used to estimate 'in-vivo' the regional electrical conductivities of the main head tissues in the approach known as parametric or bounded EIT (bEIT) [2-4], or to image the internal conductivity distribution of the head, a problem known as EIT imaging or reconstruction [5]. The parametric approach is important for improving EEG source localization accuracy [6], targeting in tDCS [7], or as a baseline in dynamic EIT [5]. The scalp and the skull conductivities have been proven to have high impact on the modeling accuracy in these applications.

A head model can be obtained from structural magnetic resonance (MR) images, followed by the segmentation (usually, from three to seven tissues are differentiated). For each tissue, the conductivity is either assigned or estimated. BEIT is typically considered for the estimation of the scalp and skull conductivities, where most of the injected power is dissipated. Although, a detailed intracranial conductivity distribution can be obtained with Diffusion Tensor Imaging (DTI)[4] or MREIT [20], these techniques are not applicable for the skull conductivity estimation. The scalp and skull can be considered homogeneous and isotropic (one parameter per tissue) or anisotropic with different tangential and radial conductivities (two parameters per tissue) [4].

Once the virtual head model is built and the measurements are obtained, the model conductivities are varied to minimize the difference between the measurements and the model predictions. The computation of the scalp potentials is known as the EIT forward problem (FP). It is governed by the Poisson equation and, for complex geometries such as the human head, it can be solved using the Boundary Element Method (BEM) [2], the Finite Element Method (FEM) [4], or the Finite Difference Method (FDM) [8]. FEM and FDM allow inhomogeneities and anisotropies. On the contrary, BEM can only be used in models of nested and closed surfaces of the tissues compartments, and assumes homogeneity and isotropy in each layer. The process of fitting the bEIT data and simulations is a non-linear optimization problem. The methods for solving this problem include: the Newton method (requires up to second order derivative computations) [4], simplex search methods, and simulated annealing.

Previous bEIT estimations used three layer spherical [9] or BEM [2, 10, 11] models with point-wise or triangular electrodes and only one (the skull conductivity) unknown. A bEIT study using FEM and two unknowns was recently reported [12]. The wide range of the reported skull conductivity estimates (from 0.004 to 0.02 S/m) using bEIT and other methods [13, 14] is most likely attributed to the different models employed in those studies. Similarly, the reported scalp conductivity varies from 0.3 to 0.5 S/m, although this is based on a very low number of studies [14].

In this work we pursue three specific goals: i) provide new experimental estimations of the scalp and skull conductivity values in detailed seven tissue FEM models; ii) study the influence of the electrode modeling; and iii) study the impact of closed skull three-layer ‘BEM-like’ models on the accuracy of the bEIT estimates.

II. METHODS

All research protocols involving human subjects were approved as safe and complying with the ethical standards in the Helsinki Declaration of 1975 by Institutional Review Boards (IRB) at the data collection site (Electrical Geodesics, Inc (EGI), Eugene, OR, USA), with informed consent obtained from two subjects (S1, a 46 year old Asian male, and S2, a 52 year old Caucasian male) recruited in the studies.

A. bEIT data collection

Two subjects wearing a 128 channel EGI geodesic net with gelled electrode-to-skin contacts were positioned in a comfortable chair and 20 μ A current at the frequency of 27 Hz was administered for 3 seconds in each of 64 distinct electrode pairs. The scalp potentials were acquired and their amplitude extracted using a 256-channel array EGI EEG 300 system [3,19], as well as electrode to scalp impedances. Sensor positions were determined using the Geodesic Photogrammetry System (GPS) described in more details elsewhere [16].

B. Detailed head models construction

The reference models of soft tissues for two adult subjects were derived from retrospective T1-weighted MR images obtained with a 3T Allegra scanner (Siemens Healthcare, Erlangen, Germany). Bone structures were derived from retrospective CT scans of the same subjects recorded with a GE CT scanner (General Electrics, Fairfield, United States). The acquisition matrix was 256x256x256 with a voxel size of 1x1x1 mm in both the CT and T1 scans. The T1 MRI images were automatically segmented into seven tissue types (brain gray matter, brain white matter, cerebrospinal fluid (CSF), scalp, eyeballs, air, and skull) and the CTs were coregistered to the corresponding MRIs and GPS sensor positions using

EGI's segmentation and image processing package, BrainK [15].

Finite element (FE) tetrahedral meshes of ~ 1.4 million of elements were built from the volumetric segmentations using the iso2mesh package [17] (Fig. 1a). The isotropic and homogeneous conductivity values were assigned to each of the non scalp and non skull tissues, based on the typical literature data: 0.2, 0.33, 1.79, and 1.4 S/m for the white matter (WM), gray matter (GM), CSF, and eye balls [14]. The FEM was used for computing the EIT FP. As described in [4], the electrical problem is reduced to a linear system of equations, where \mathbf{K} is the 'stiffness' matrix containing the structural and conductivity information, \mathbf{V} is the unknown potential vector at each node of the mesh, and \mathbf{I} is an independent vector that considers the boundary conditions. The linear system was solved using a preconditioned conjugate gradient algorithm [18].

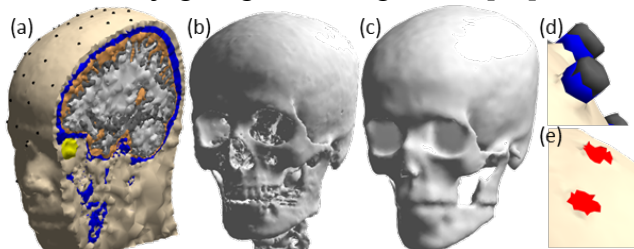


Fig. 1 (a) Computational head model for subject 1 (S1), segmentation, FE mesh, and pointwise electrodes. (b) Skull of the pointwise, volumetric, and CEM models. (c) Skull of the closed skull and closed skull – no CSF models. (d) Detailed volumetric electrode model. (e) Portion of the outer surface with different boundary conditions in the CEM model (in red).

Within the detailed head model shown in Fig. 1a for subject 1, we studied three variations of electrode modeling:

Pointwise: each electrode is a node of the tetrahedral mesh. \mathbf{I} is an all zero vector except for two elements: the nodes corresponding to the current injection electrode pair.

Volumetric: the electrodes are modelled as small cylinders of 1 cm height and 5mm radius placed on the scalp. Each cylinder is composed by a thin layer of scalp (2mm) because of suction, a layer of conductive gel (4mm, 1.5 S/m), and metal (4mm, 500 S/m), as shown in Fig. 1d. The FEM is solved

as in the pointwise case, but in this model, current sources and sinks are placed in the metal layers.

CEM: the specific boundary conditions are imposed in the electrode areas (see Fig. 1e) in contact with the scalp, modifying the FEM linear system of equations. The CEM boundary conditions take into account the electrode to skin contact impedance. The details of the CEM can be found elsewhere [5].

For subject 1, two other model variations were analyzed:

Closed skull: this model is composed by five nested and closed surfaces (scalp, skull, CSF, GM, and WM) and pointwise electrodes. This model is similar to five-layer BEM models. The skull layer is shown in Fig. 1c.

Closed skull – no CSF: this model is the same as previous model except that the conductivity of the CSF layer is set equal to the GM conductivity (0.33 S/m). It is similar to three-layer BEM models where the CSF is not considered.

C. Nonlinear optimization method

For each current injection pair, the estimation process can be formulated as an optimization problem:

$$(1)$$

where σ_s and σ_{sk} are the scalp and skull conductivity values, \mathbf{V} is the simulated potential at the electrodes, and \mathbf{M} is the vector with the measurements. Note that expression (1) is equivalent to the maximum likelihood estimator assuming uncorrelated white Gaussian noise [4]. We used the Newton method to estimate \mathbf{V} and from (1). This method requires the first and second order derivatives of \mathbf{V} with respect to \mathbf{I} and \mathbf{M} . The computation of these derivatives for the pointwise and volumetric models is detailed in [4]. The formulation of the derivatives for the CEM model were derived specifically for this work in an analogous way.

III. RESULTS

Two injection pairs out of 64 were identified as “bad” channels and were discarded. The electrode to skin impedances for the CEM case were the same as measured in the bEIT experiment. For each head model, the conductivity estimations were performed for each of the remaining 62 bEIT injection pairs separately. The optimization in Eq. (1) was set to stop after 10 iterations of the Newton method as it was usually stagnated in 7 or 8 iterations. The initial values were set as 0.2 and 0.001 S/m (plus some small random variations) for the scalp and skull conductivities. Lower initial than expected values helps to the convergence of the method [4]. For some particular pairs, depending on the particular model, the method did not converge, converged to negative values, or estimated meaningless results. The number of these “outlier” cases was not more than 8 out of 62, and were discarded.

Fig. 2a (Fig. 2b) shows in a box plot the scalp (skull) conductivity estimations for all current injection pairs obtained within each model. Table 1 summarizes the averaged results, and, for each subject, the number of estimations that resulted in a better fitting for each model. A better fitting means a lower norm of the difference between the measurements and the EIT FP computed with the estimations.

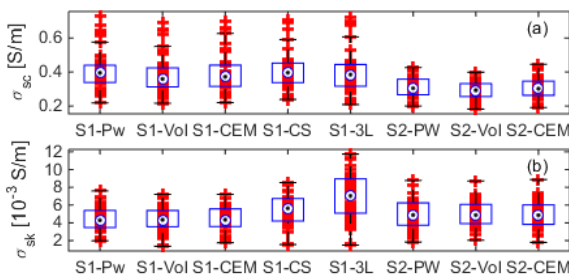


Fig. 2 (a) Scalp and (b) skull conductivity estimations for S1 and S2, for pointwise (Pw), volumetric (Vol), CEM, closed skull (CS), and closed skull – no CSF (3L) models. Red crosses represent individual estimations for each current injection pair, central marks indicate the median, and box edges are the 25th and 75th percentiles.

Table 1 Averaged scalp (SC) and skull (SK) conductivity estimations [S/m], and number of pairs (P) with best fitting for both subjects.

Models	S1-SC	S1-SK	S2-SC	S2-SK	S1-P	S2-P
Pointwise	0.401	0.00443	0.310	0.310	2	13
Volumetric	0.378	0.00439	0.292	0.292	18	28
CEM	0.389	0.00447	0.305	0.305	26	13
Closed skull (CS)	0.412	0.00550			2	
CS – no CSF	0.394	0.00705			5	

IV. DISCUSSION

Measured conductivity values: the estimated scalp conductivity is in the middle range of the reported values by other similar studies, but the estimated skull conductivity is in the lower limit of the reported range. In addition to the different subject pools and intersubject variability, some significant difference might be due to the different models used in each study. In [9], the very first estimations were performed in a quite simple model: a three layer concentric sphere. In [10], with a three layer BEM model and pointwise electrodes, the skull conductivity estimation (~ 0.01 S/m) was similar to the later studies, but scalp estimation was lower (~ 0.2 S/m), probably due to BEM pointwise electrode modelling. Then, in [2], the BEM model used triangles for the electrodes instead of nodes, and the estimated scalp and skull conductivities were ~ 0.33 S/m and ~ 0.008 S/m, respectively. In [11], a similar three layer BEM model was used but the scalp and intracranial conductivities were fixed to 1S/m, thus, a one parameter estimation was performed with a result of the scalp/skull conductivity ratio to be ~ 0.04 . Lastly, FEM was used in [12] in a 2D search, with CSF included, resulting in estimates ~ 0.008 S/m for the skull and a rather high value (0.6S/m) for the scalp. We believe that significant variance the skull conductivity estimations reported in the literature so far can be attributed to the modelling factors. For this reason, we analyzed the impact of the electrode modelling, the influ-

ence of a closed ‘BEM-like’ skull, and the influence of not considering the CSF layer (similar to a three-layer BEM model).

Differences between estimations can be also explained by inter-subject variability and age [14]. In our results, the scalp conductivity difference between both subjects is expected, as S2 is hairless. A hairless scalp is usually dryer and thus, less conductive. On the other hand, the skull thickness in S1 is lower than in S2, implying less spongy bone (more conductive than compact bone) and a less conductive skull.

Influence of the electrode model: the use of pointwise, volumetric, or CEM electrode models resulted in a small difference (<6%) across different estimations of the scalp, and even smaller (<2%) for the skull conductivities. However, volumetric and CEM models showed, in most cases, a better fitting between measurements and simulations.

Influence of a closed skull: a closed skull resulted in an approximately high (23%) overestimation of the skull conductivity. This is expected if the skull holes are not modelled, as the estimated skull conductivity has to be higher to compensate for them, i.e., the skull has to be ‘more transparent’ for the current. This effect might partially explain the higher skull conductivity estimation of previous studies.

Influence of CSF: assuming CSF conductivity equal to GM conductivity led to an extra 28% of skull conductivity overestimation. Adding together these two effects resulted in a skull conductivity estimation of ~ 0.007 S/m for S1, very close to literature bEIT three-layer BEM estimates.

V. CONCLUSIONS

We estimated scalp (skull) conductivities in two subject to be 0.3 (0.005) and 0.4 (0.0045) S/m correspondingly. Different electrode models showed no significant differences in the estimations, but CEM and volumetric electrode models

resulted in a better fitting between data and predictions. A closed skull showed a significant overestimation of the skull conductivity value. Neglecting the CSF layer also produces an additional and significant skull conductivity overestimation. It is likely that the combination of both modelling simplifications explain the lower skull conductivity estimated in this study using a detailed FEM model, compared to previous similar studies with simpler BEM models.

The results of this preliminary study should be validated with experiments in more subjects, and also more accurate skull models including spatial inhomogeneities should be analyzed. Finally, the impact of the brain conductivity set to the literature typical values in this study needs to be examined as well.

ACKNOWLEDGMENT

This work was supported by the ANPCyT PICT 2011-11-0909, UNLP 11-I-166, CONICET, CIC-pBA, the Fulbright Foundation, USA, the Fundación Bunge & Born, Argentina, and the National Institute of Mental Health (Grant R44MH106421). The discussions with the EGI team, in particular, Phan Luu, Erik Anderson and Colin Davis are acknowledged.

CONFLICT OF INTEREST

Turovets and Tucker are employees of Electrical Geodesics, Inc., a manufacturer of dense array EEG systems.

REFERENCES

1. Bayford, R.H. (2006) Bioimpedance tomography (electrical impedance tomography). *Annu. Rev. Biomed. Eng.* 8:63-91.
2. Gonçalves, S.I., et al. (2003) In vivo measurement of the brain and skull resistivities using an EIT-based method and realistic models for the head. *IEEE Trans. Biomed. Eng.* 50(6):754-767.
3. Turovets, S.I., et al. (2008) Conductivity analysis for high-resolution EEG, *BMEI 2008*. vol. 2, pp 386-393.
4. Fernández-Corazza, M., et al. (2013) Analysis of parametric estimation of head tissue conductivities using Electrical Impedance Tomography. *Biomed Signal Proces* 8(6):830-837 DOI: 10.1016/j.bspc.2013.08.003.
5. Lionheart, W.R.B., N. Polydordes, and A. Borsic, (2004) *Electrical Impedance Tomography: Methods, History and Applications*. Inst. Phys., D.S. Holder, Editor, pp 3-64.
6. Vanrumste, B., et al. (2000) Dipole location errors in electroencephalogram source analysis due to volume conductor model errors. *Med Biol Eng Comput* 38:528-534.
7. Opitz, A., et al. (2015) Determinants of the electric field during transcranial direct current stimulation. *NeuroImage* 109:140-150 DOI: 10.1016/j.neuroimage.2015.01.033.

8. Turovets, S., et al. (2014) A 3D Finite-Difference BiCG Iterative Solver with the Fourier-Jacobi Preconditioner for the Anisotropic EIT/EEG Forward Problem. *Comp. Math. Methods in Medicine*:1-12.
9. Eriksen, K.J. (1990) In vivo human head regional conductivity estimation using a three-sphere model, *Proc. of the Annual Conf. on Engineering in Medicine and Biology*. pp 1494-1495.
10. Oostendorp, T.F., J. Delbeke, and D.F. Stegeman (2000) The conductivity of the human skull: results of in vivo and in vitro measurements. *IEEE Trans Biomed Eng* 47(11):1487-1492.
11. Clerc, M., et al. (2005) In vivo conductivity estimation with symmetric boundary elements, *NFSI2005*. vol. 7.
12. Ouypornkochagorn, T., N. Polydorides, and H. McCann. (2014) In Vivo Estimation of the Scalp and Skull Conductivity, *EIT2015*. pp 10-10.
13. Hoekema, R., et al. (2003) Measurement of the Conductivity of Skull, Temporarily Removed During Epilepsy Surgery. *Brain Topogr* 16:29-38.
14. Horesh, L. (2006) Some Novel Approaches in Modelling and Image Reconstruction for Multi-Frequency Electrical Impedance Tomography of the Human Brain. PhD Thesis, University College London.
15. Li, K., A.D. Malony, and D.M. Tucker. (2006) Automatic brain MR image segmentation by relative thresholding and morphological image analysis, *VISAPP (1)'06*. pp 354-364.
16. Russell, G.S., et al. (2005) Geodesic photogrammetry for localizing sensor positions in dense-array EEG. *Clin Neurophysiol* 116(5):1130-1140 DOI: 10.1016/j.clinph.2004.12.022.
17. Fang, Q. and D.A. Boas. (2009) Tetrahedral Mesh Generation from Volumetric Binary and Gray-scale Images, *Proc. of the Sixth IEEE International Conference on Symposium on Biomedical Imaging: From Nano to Macro*. Piscataway, NJ, USA pp 1142-1145.
18. Barrett, R., et al., (1994) *Templates for the Solution of Linear Systems: Building Blocks for Iterative Methods*, 2nd Edition. SIAM, Philadelphia, PA.
19. Esler, B., et al. (2010) Instrumentation for low frequency EIT studies of the human head and its validation in phantom experiments. *J Phys Conf Ser* 224(1):012007-012007.
20. Hyung Joong Kim, Oh In Kwon and Eung Je Woo. Regional absolute conductivity reconstruction using projected current density in MREIT. *Phys. Med. Biol.* 57 (2012) 5841–5859
21. Zhang, Y., W. van Drongelen, and B. He, “Estimation of in vivo brain-to-skull conductivity ratio in humans”, *Applied Physics Letters*, vol. 89, pp. 223903-1–3, 2007.

Author: Mariano Fernández Corazza
 Institute: LEICI, Facultad de Ingeniería, Universidad Nacional de La Plata
 Street: Calle 48 y 116
 City: La Plata
 Country: Argentina
 Email: marianof.corazza@ing.unlp.edu.a